



Effects of Shape Memory Alloys on Response of Steel Structural Buildings within Near Field Earthquakes Zone

Mahmoud Ahmadinejad ^a, Alireza Jafarisirizi ^b, Reza Rahgozar ^{c*}

^a Civil Engineering Department, Sharif University of Technology International Campus, Kish Island, Iran.

^b Ph.D. Candidate at Civil Engineering Department, Shahid Bahonar University of Kerman, Kerman, Iran.

^c Civil Engineering Department, Shahid Bahonar University of Kerman, Kerman, Iran.

Received 05 February 2020; Accepted 19 June 2020

Abstract

Base isolation is one of the effective ways for controlling civil engineering structures in seismic zone which can reduce seismic demand. Also is an efficient passive control mechanism that protects its superstructure during an earthquake. However, residual displacement of base-isolation systems, resulting from strong ground motions, remain as the main obstacle in such system's serviceability after the earthquake. Shape Memory Alloys (SMA) is amongst the newly introduced smart materials that can undergo large nonlinear deformations with considerable dissipation of energy without having any permanent displacement afterward. This property of SMA may be utilized for designing of base isolation system to increase the structure's serviceability. Here, a proposed semi-active isolation system combines laminated rubber bearing system with shape memory alloy, to take advantage of SMAs high elastic strain range, in order to reduce residual displacements of the laminated rubber bearing. Merits of the system are demonstrated by comparing it to common laminated rubber bearing isolation systems. It is found that the optimal application of SMAs in base-isolation systems can significantly reduce bearings' residual displacements. In this study, OpenSees program for a three dimensional six-storey steel frame building has been used by locating the isolators under the columns for investigating the feasibility of smart base isolation systems, i.e., the combination of traditional Laminated Rubber Bearing (LRB) with the SMA, in reducing the structure's isolated-base response to near field earthquake records are examined. Also, a new configuration of SMAs in conjunction with LRB is considered which make the system easier to operate and maintain.

Keywords: Base Isolation; Shape Memory Alloys; Steel Structure; Near Field Earthquakes; Nonlinear Seismic Analysis.

1. Introduction

Earthquake is one of the most destructive phenomena which caused catastrophic destruction. Annually, earthquakes take thousands lives, and bring about significant financial loss all over the world. Today, civil engineers concern is to design structures to withstand under earthquake forces and to dissipate the input earthquake energy through in-elastic deformations [1]. Generally, structures are designed according to codes with criteria based on structural collapse prevention. This approach allows for the forces due to ground motion to be transmitted into the structure; and relies only on strength and ductility of the structure to resist these forces. Hence, large motion can occur at higher floors of the structure, causing severe damage to the building. Seismic base isolation system change structure's response by allowing the ground to undergo relatively large displacements without transmitting forces into the isolated structure. In fact, in most isolation designs, the structure generally moves as a rigid body. This means that ground accelerations

* Corresponding author: rahgozar@uk.ac.ir

 <http://dx.doi.org/10.28991/cej-2020-03091550>



© 2020 by the authors. Licensee C.E.J, Tehran, Iran. This article is an open access article distributed under the terms and conditions of the Creative Commons Attribution (CC-BY) license (<http://creativecommons.org/licenses/by/4.0/>).

signals that pass through the isolators remains relatively constant along structure's height [2], i.e. the acceleration of the top floors differ slightly from the accelerative motion imposed at lower level. It has been pointed out by Markris and Aghagholizadeh (2019), for reducing the earthquake forces acting on a structure or to absorb a part of the seismic energy, innovative systems and devices have been developed [3]. Seismic isolation systems are able to reduce the natural frequency created by the seismic load applied to the structures. Over the last few decades, several types of seismic isolators have been proposed and developed and are often divided into elastomeric and friction isolators, i.e. low damping natural rubber bearing, lead rubber bearing, high damping natural rubber bearing, pure- friction and friction pendulum system [4, 5]. Several studies have also focused on the evaluation of the seismic performance of highway bridges with seismic isolators using yielding steel dampers and laminated rubber bearings in comparison with other popular isolation systems [6, 7].

Recently, advanced materials have been used for seismic isolator and damping systems [8]. A group of metals that have the ability to dissipate energy through repeated cyclical loading, without significant permanent deformations is known as Shape Memory Alloys (SMAs). It has been pointed out by Wesolowskyi and Wilson (2004), shape memory alloys as compared to other metals, have a wide usable strain range; up to about 8%; thus, requiring a smaller volume of material in order to produce the comparable damping capacity. Furthermore, they have needed ability, i.e. providing stiff elastic resistance under large displacements [9]. A numerical parametric study carried out by Asgharian *et al.* (2016) for self-centering hybrid damper [10]. In this study, steel pipe used as a vertical link for energy dissipation and two transverse pairs of shape memory alloy wires as for re-centering components. Tian *et al.* (2018) used shape memory alloy tuned mass damper for seismic vibration control of power transmission tower in order to assess nonlinear time history analysis method [11]. Ghasemi *et al.* (2019) pointed out that as the shape memory alloy is highly capable of dissipation energy, which can control the vibrations created by wave-induced of the offshore jacket platforms [12]. Also base isolation systems can have an extensive applications in different types of tall structures in order to reduce the lateral displacements, drifts and natural frequencies [13, 14].

In this study, a three dimensional six storey steel frame building has been considered. The base isolation system has been design according to ASCE7 code requirements. Their characteristics dependent on the weight and period of its superstructure. The near field earthquake data from Northridge records are selected and scaled in order to carry the response history analysis; by generating design response spectrum which is specialized for the site. The structure is modeled in OpenSees package, which is based on finite element method. By defining the base isolation materials from OpenSees library, fixed-based structure and base isolation system in a 3D model are analysed. SMA bars are implemented into the base isolation system's model and the structural response due to earthquake records are computed and compared.

2. Base Isolation and Shape Memory Alloys Concept

Shape memory alloys are earthquake-resistant in civil engineering structures which can dissipate significant energy and are able to return to their previous shape after being severely deformed. It has been pointed out by Nakashima *et al.* (2004) that designing of base isolation in any structures should follows two objectives, achieving life safety and limiting damage due to a significant earthquake [15]. To achieve these objectives, the base isolation should be stable and sustain forces and displacements with significant earthquake [16]. Base isolation system has a limited ductility and a significant inelastic response which meet the second performance objective of damage control [17, 18]. A lead rubber bearing, manufactured from layers of rubber, bonded with layers of steel and in middle of bearing a solid lead core ted shown in Figure 1 [19].

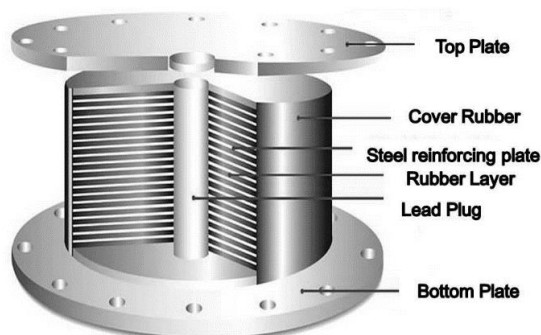


Figure 1. Lead rubber bearing [19]

Design of isolators is based on the ASCE7, the following procedures such as equivalent lateral static force and dynamic analysis for time-history can be used. For design of isolators, some requirements such as structural site with S_I and site class A, B, C, or D. Effective period of isolated structure at the maximum displacement, T_M , and the effective period of the isolated structure at the design displacement, T_D , can be obtained [20]. Also, the base isolation system should meet the following criteria [21]:

- Effective stiffness at the design displacement is greater than one-third of the effective stiffness at 20 percent of the design displacement.
- Base isolation system is capable of producing a restoring force.
- Maximum considered earthquake displacement to less than the total maximum displacement.

The following steps are illustrated for dynamic analysis procedure:

- First step: the target period assumed to be not less than at least three times of the fixed base period of structure ($T_D > 3 T_{fix}$).
- In the second step, design displacement (D_D) and maximum considered earthquake response displacement (D_M), at the center of rigidity of the isolation system can be calculated by Equations 1 to 4.

$$D_D = \frac{g \cdot S_{D1} \cdot T_D}{4\pi^2 \cdot B_D} \quad (1)$$

$$D_M = \frac{g \cdot S_{M1} \cdot T_M}{4\pi^2 \cdot B_M} \quad (2)$$

Where [11]:

$$T_D = 2\pi \sqrt{\frac{W}{K_{Dmin} \cdot g}} \quad (3)$$

$$T_M = 2\pi \sqrt{\frac{W}{K_{Mmin} \cdot g}} \quad (4)$$

Where; W : weight of structure above the base isolator. Where K_{Dmin} : minimum effective stiffness of base isolation at the design displacement in the horizontal direction and K_{Mmin} : minimum effective stiffness of base isolation at the maximum considered earthquake response displacement in the horizontal direction can be obtained by Equations 5 and 6 respectively:

$$K_{Dmin} = \frac{\sum |F_D^+|_{min} + \sum |F_D^-|_{min}}{2D_D} \quad (5)$$

$$K_{Mmin} = \frac{\sum |F_D^+|_{min} + \sum |F_D^-|_{min}}{2D_M} \quad (6)$$

As shown in Equations 5 and 6, minimum effective stiffness of the isolators can be obtained by using parameters such as $\sum |F_D^+|_{min}$ & $\sum |F_D^-|_{min}$ from testing the isolators, so value for T_M , can be assumed to be 3.0 sec.

- Second step: the modified displacement can be obtained using Equations 7 and 8.

$$D_D' = \frac{D_D}{\sqrt{1 + \left(\frac{T_{fix}}{T_D}\right)^2}} \quad (7)$$

$$D_M' = \frac{D_M}{\sqrt{1 + \left(\frac{T_{fix}}{T_M}\right)^2}} \quad (8)$$

- Third step: the total of design displacement and maximum considered earthquake response displacement (D_{TD} and D_{TM}), can be obtained by Equations 9 and 10 respectively:

$$D_{TD} = D_D' \left[1 + y \frac{12e}{b^2 + d^2} \right] \quad (9)$$

$$D_{TM} = D_M' \left[1 + y \frac{12e}{b^2 + d^2} \right] \quad (10)$$

- Fourth step: the base shear can be evaluated using Equations 11 and 12.

$$V_s = \frac{K_{Dmax} D_D}{R_I} \quad (11)$$

$$K_{Dmax} = \frac{1 + \alpha}{1 - \alpha} K_{Dmin} \quad (12)$$

Where; α is the ratio of secondary stiffness to primary stiffness of isolator.

The R_I factor is based on the type of seismic force-resisting system used for the structure above the isolation system and should be 0.375 of the value of R given in ASCE 7, Table 12.2-1, with a maximum value not greater than 2.0 and a minimum value not less than 1.0. It should be noted that in this study the isolated structure $R_I = 2$.

- Fifth step: controlling drift and base shear limit which shall not exceed the following limits:

1. Maximum storey drift of the structure above the isolation system shall not exceed $0.015h_{sx}$.
2. Maximum storey drift of the structure above the isolation system shall not exceed $0.020h_{sx}$.

The value of base shear, V_s shall not be taken as less than one of the following limits:

1. Base shear corresponding to the factored design wind load.
2. Lateral seismic force required to fully activate the isolation system multiplied by 1.5.

The isolators make a reduction in forces created by earthquake in the design of structures and also reduce floor displacement and accelerations which can be apply into the new and retrofitting of existing structures. Recently, the performance of the isolator in the base of structures has been used in near-fault earthquakes, long period and large velocity pulses in the velocity history of ground motion can be characterized. For the isolated base structure, if the period of the mentioned pulses coincides with the period of the structure, the seismic response of the system will be amplified. The base isolation structure will be influenced with normal to the fault ground motion such that, the isolator effects will be reduced or maybe negative. To solve this type of problems with the isolation systems, shape memory alloys can be applied in vibration control of structures. The shape memory alloys has two unique properties: shape memory effect and super elastic effect. Both of these properties acting on the solid-solid phase transformation first more ordered phase named austenite and less ordered phase named martensite. To transfer from the one mentioned phase to another, it is necessary to exist the variation in temperature or stress which the transformation due to temperature variation called shape memory effect and due to the stress variation called super elastic effect.

The super elastic effect can be considered in base isolator residual displacement problem. It can fully reenter the original shape of the isolator, and this shape recovery is also compeer with significant hysteresis loop which leads to energy dissipation. Combination of the isolators and these smart materials can lead to an intelligent solution for the mentioned problems with isolators in a near-fault earthquake. Residual displacements of the isolators can be removed with a re-centring force which was generating by the SMA bars due to the ground motion. In this study to meet the mentioned purpose, two principal part of isolators (top and below flange of isolator) should be linked with the SMA bars as shown in Figure 2.

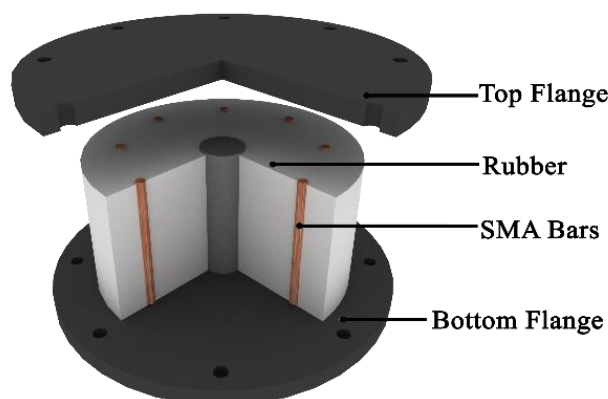


Figure 2. Combination LRB isolators with the SMA bars

Several key parameters on the hysteresis loop have be determined for shape memory alloys as illustrated and shown in Figure 3 which indicate the energy dissipation and restoration after unloading.

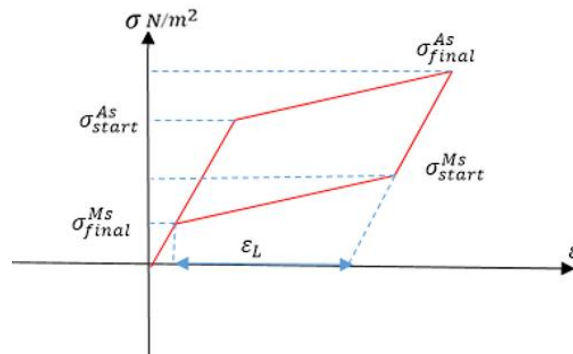


Figure 3. Stress-strain behavior of the shape memory alloys [21]

σ_{start}^{As} : Starting stress value for the forward phase transformation

σ_{final}^{As} : Final stress value for the forward phase transformation

σ_{start}^{Ms} : Starting stress value for the reverse phase transformation

σ_{final}^{Ms} : Final stress value for the reverse phase transformation

ϵ_L : Maximum residual strain

α : Parameter for material responses in tension and compression.

3. Time History Analysis and Structural Model

As suggested by ASCE 7, in time-history analysis, at least three different strong ground motions will be needed to apply the structural model and the scaled ground motion [21]. Seven ground motions which are the maximum value of each response parameter have been used for design as listed in Table 1, are taken for the response- history analysis. All of the selected records are near field record as shown in Table 1.

Table 1. Description of records [17]

Event's name	Date	V_s (m/s)	Fault distance (KM)
1. Chi Chi Taiwan	1999	472.8	5.18
2. Northridge	1999	282.3	6.5
3. Cope Mendocino	1992	712.8	8.18
4. Loma Prieta	1989	1070.3	5.02
5. Tabas	1978	766.8	2.05
6. Erzincan	1992	274.5	4.38
7. Landers	1992	684.9	2.19

In this study several combinations of scaling factors have been defined for three 6-storey structural models and assumed to be located in California zone. The details of steel structural building are shown in Figures 4 and 5 and other properties are listed below:

- No. storey: 6
- Height of stories: 3.2 m
- No. span in X direction: 3
- No. span in Y direction: 2
- Span length in X & Y direction: 6 m
- Lateral load resisting system in X & Y direction: Special Moment Frame
- Dead load: 350 Kg/m² for each storey and 250 Kg/m² for roof
- Live load: 150 Kg/m² for each storey and 200 Kg/m² for roof
- Circumferential wall: 800 Kg/m for each storey and 250 Kg/m for roof

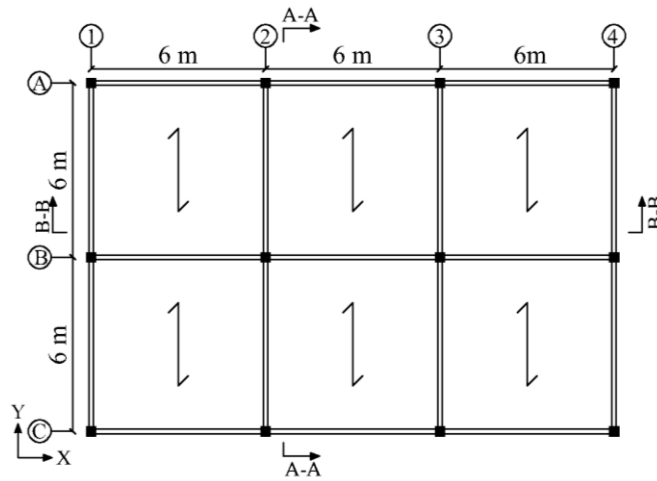


Figure 4. Plan of 6-storey model

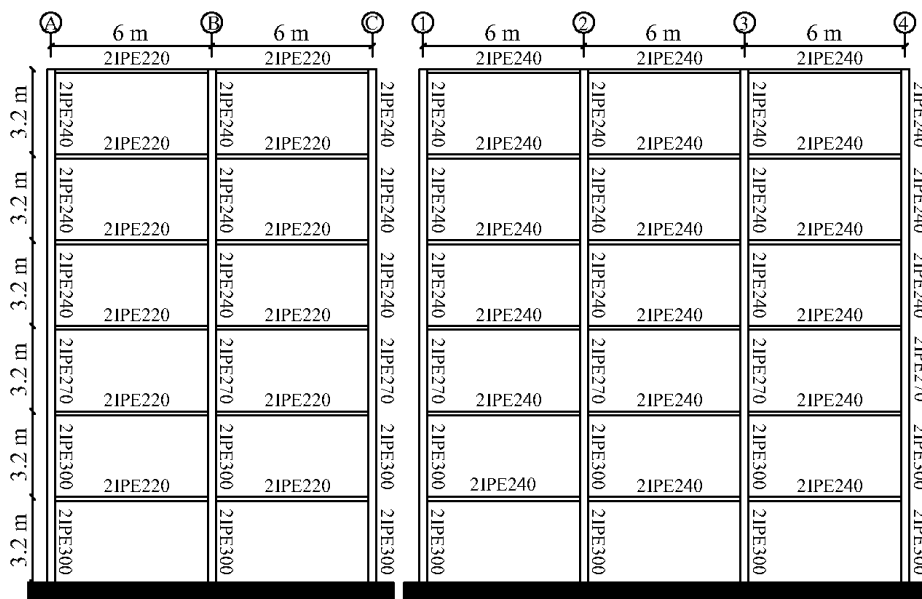


Figure 5. Beams and columns of 6-storey model in X & Y direction

The dynamic properties of steel building are listed in Table 2.

Table 2. 6-storey model, dynamic properties (Natural period in sec)

Number of Mode	X direction	Y direction	Rotational
I	0.64	0.53	0.42
II	0.2	0.17	0.14
III	0.11	0.09	0.07

The site class of soil considered to be C (very dense soil and soft rock) base on ASCE 7 code, and is residential structures. The design parameters for the models are as follow [21]:

Importance Factor (I_e) was defined as 1 in this study concerning the risk category.

Site location, evaluate S_I and S_S (acceleration parameters), $S_I = 0.82g$ and $S_S = 1.61g$

Site class, to evaluate properties of soil at a given site.

Site categorized are as site class A, B, C, D, E and F.

For this study site classification C has been selected (C: Very dense soil and soft rock).

F_a and F_v are functions of the site class and site coefficient parameters can be determined by acceleration parameters and site classification:

$$S_I = 0.82g \quad S_S = 1.61g \quad \text{Soil Type (site classification): } C$$

Based on the ASCE 7:

$$F_a: \text{ Site coefficient at short periods } \Rightarrow F_a = 1$$

$$F_v: \text{ Site coefficient at 1 second period } \Rightarrow F_v = 1.3$$

Maximum considered earthquake response spectral (MCE_R), response acceleration parameters adjusted for site class effects can introduce by Equation 13:

$$S_{MS} = F_a \cdot S_S = 1 * (1.61g) = 1.61g \tag{13}$$

Design earthquake spectral response acceleration parameter at a short period, S_{DS} , and at the 1 second period, S_{D1} , can calculated using Equations 14 and 15.

$$S_{DS} = 0.667 S_{MS} \tag{14}$$

$$S_{D1} = 0.667 S_{M1} \tag{15}$$

S_{DS} : 5% damped design spectral response acceleration at 0.2 second period

S_{D1} : 5% damped design spectral response acceleration at 1 second period

$$S_{DS} = 0.667 S_{MS} = 0.667 \times 1.61g = 1.0733g$$

$$S_{D1} = 0.667 S_{M1} = 0.667 \times 1.066g = 0.71066g$$

Base on ASCE 7, the risk category are listed in Tables 3 and 4 [21].

Table 3. Risk category based on the short period [21]

Value of SDS	Risk category		
	I or II	III	IV
$S_{DS} < 0.167g$	A	A	A
$0.167g \leq S_{DS} < 0.33g$	B	B	C
$0.33g \leq S_{DS} < 0.5g$	C	C	D
$0.5g \leq S_{DS}$	D	D	D

Table 4. Risk category based on the S period [21]

Value of SD1	Risk category		
	I or II	III	IV
$S_{D1} < 0.067g$	A	A	A
$0.067g \leq S_{D1} < 0.133g$	B	B	C
$0.133g \leq S_{D1} < 0.2g$	C	C	D
$0.2g \leq S_{D1}$	D	D	D

For moment resisting frames category (D), behavior factor of (R) = 8 and the seismic response coefficient, C_s , can be obtained using Equation 16.

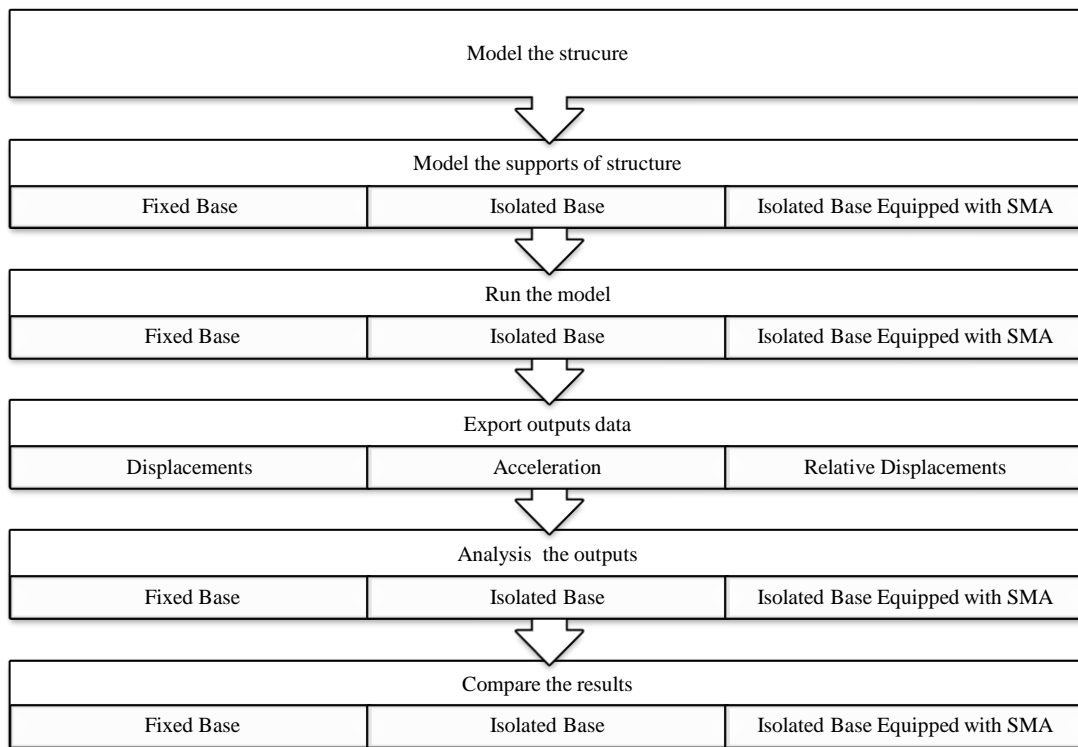
$$C_s = \frac{S_{DS}}{\frac{R}{I_e}} \quad C_s = \frac{2.49g}{\frac{8}{1}} = 0.13416g \tag{16}$$

The approximate fundamental period (T_a), in s, can be calculated by Equation 17.

$$T_a = C_t \cdot h_n^x \tag{17}$$

Where h_n is the structural height from the base, C_t and x are determined from ASCE 7 [21].

The following flowchart is given to show procedures of research methodology:



4. Results and Comparisons

In this study, displacement and acceleration responses of the model have been presented and compared with each other in such a ways to illustrate the significant differences which exist in displacement and acceleration responses between the fixed base and isolated base and isolated base equipped by shape memory alloys material in isolators:

4.1. Fixed Base Results

Displacement response for an ordinary building subjected to Northridge record is shown in Figures 6 to 9.

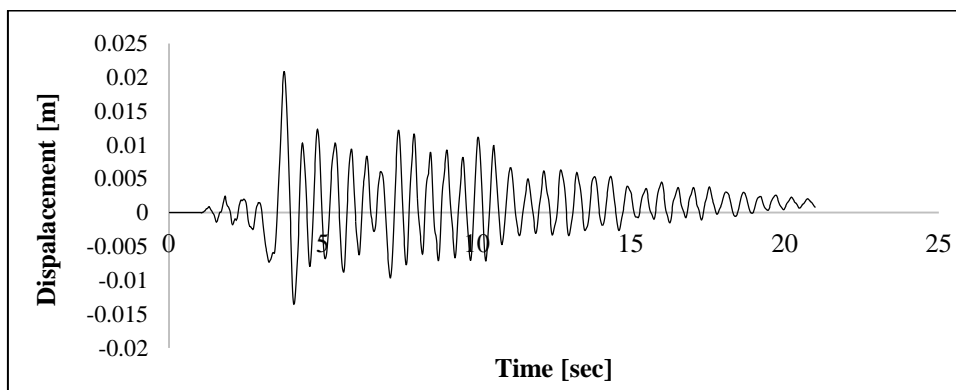


Figure 6. X-Direction displacement response of first floor for Northridge record

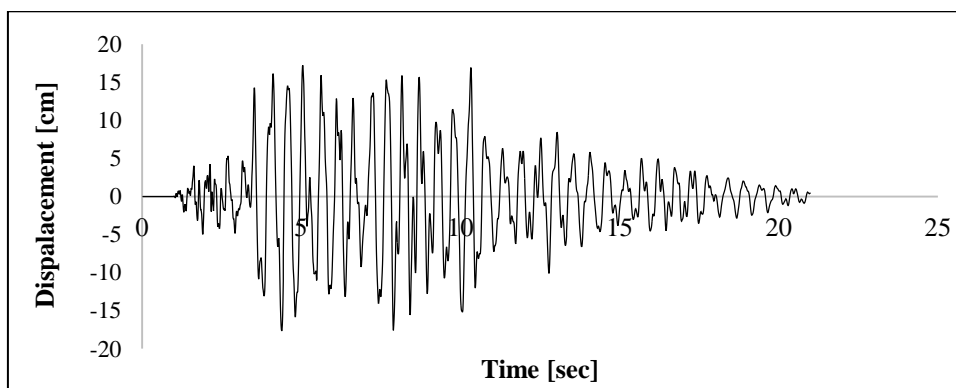


Figure 7. X-Direction displacement response of sixth floor for Northridge record

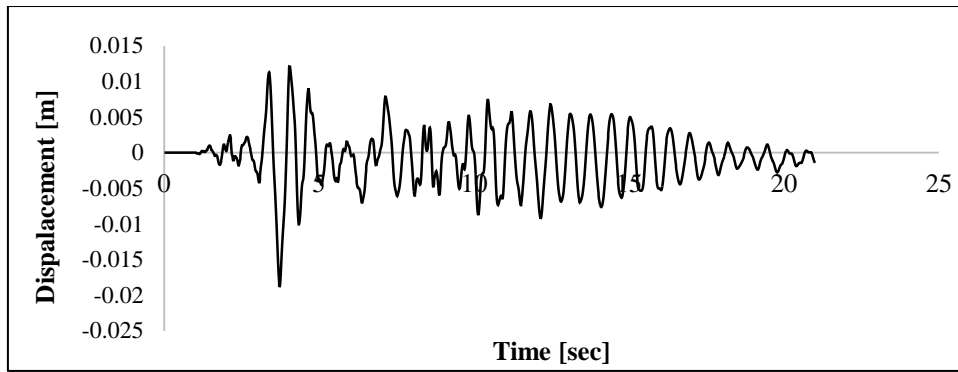


Figure 8. Y-Direction displacement response of first floor for Northridge record

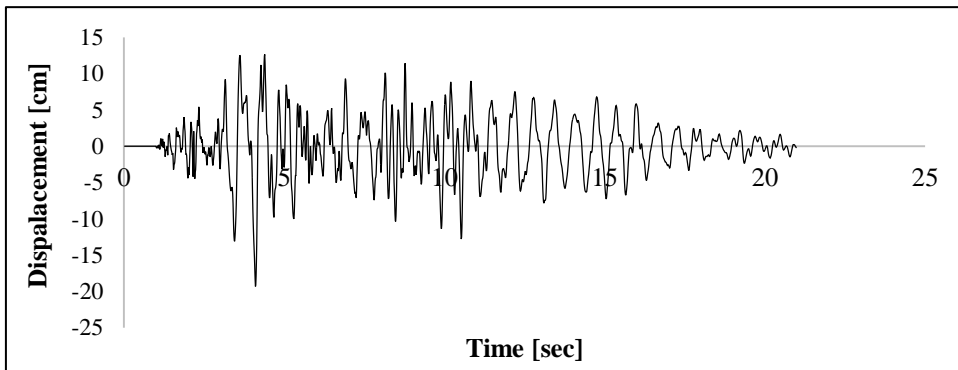


Figure 9. Y-Direction displacement response of sixth floor for Northridge record

According to Figures 6 to 9, in a 6-storey steel structure, displacement graphs demonstrate a response for an ordinary building where the maximum displacement in the first storey is 2.09 cm and 1.88 cm in X and Y directions. In sixth storey, maximum displacement is 17.6 cm and 19.3 cm in X and Y direction respectively. So, the building has a noticeable relative displacement in stories. The period of the structure is same as conventional steel moment frames.

4.2. Isolated Base Results

Displacement response for an ordinary building subjected to Northridge record is shown in Figures 10-13.

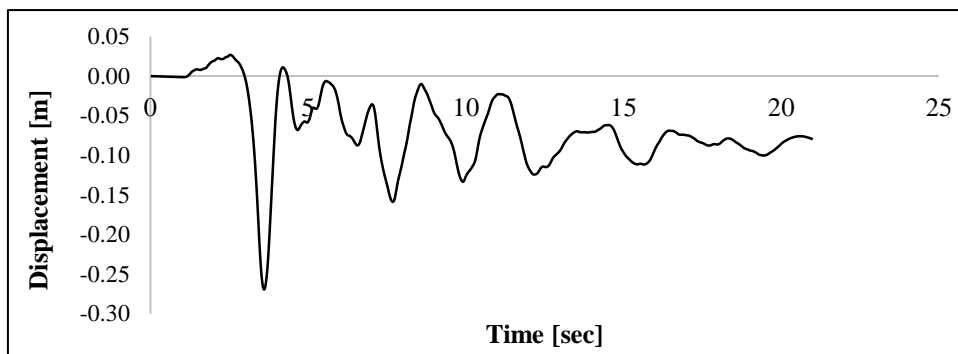


Figure 10. X-Direction displacement response of first floor to the Northridge record

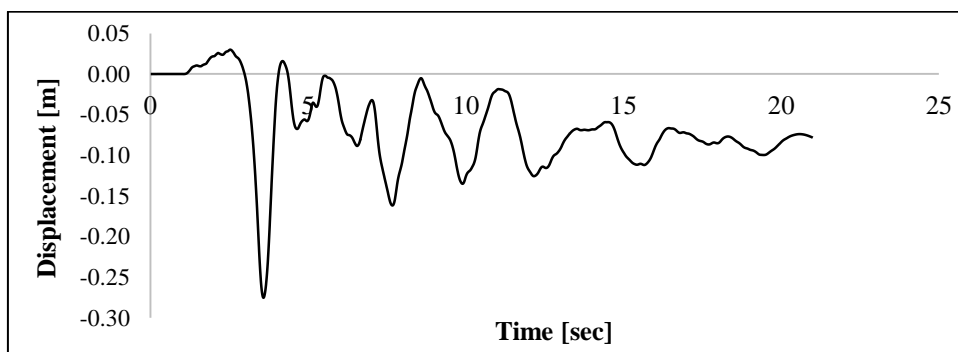


Figure 11. X-Direction displacement response of sixth floor to the Northridge record

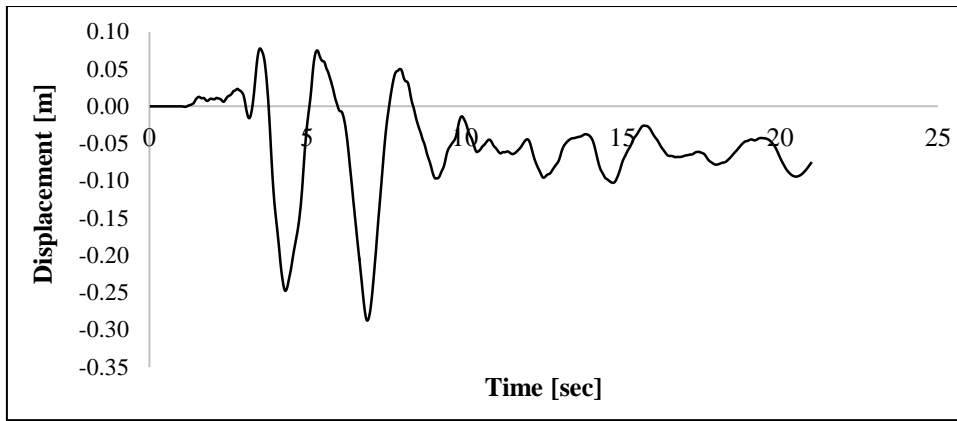


Figure 12. Y-Direction displacement response of first floor for Northridge record

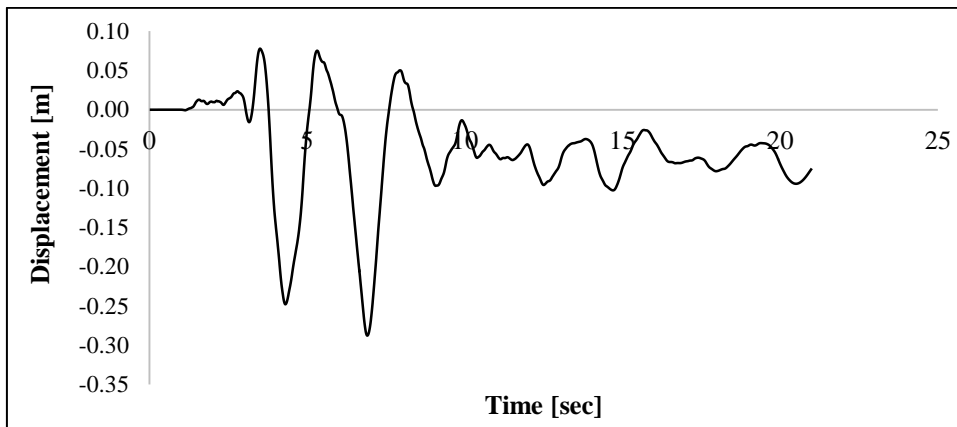


Figure 13. Y-Direction displacement response of sixth floor for Northridge record

Compared to the fixed base, the relative displacement decreased from 4.02 cm to 0.59 cm and from 3.17 cm to 0.83 cm in X and Y direction respectively. The relative displacement shown in Figure 14, indicate a reduction since isolators have been used. However, after earthquake, a significant residual displacement can be observed in base isolation devices, which consequently alter the performance of the isolators afterwards.

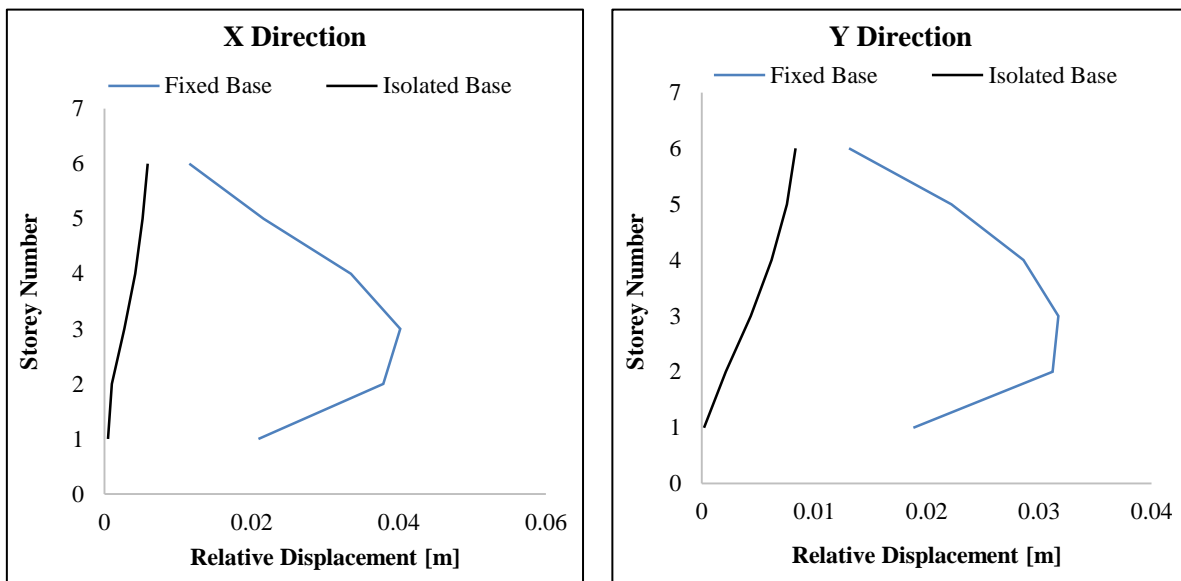


Figure 14. X & Y Direction relative displacement of each floors for Northridge record

4.3. Isolated Base Equipped with SMA Results

As observed in the base isolation system, there is a negligible residual displacement compare to the base-isolated system equipped with shape memory alloys, the residual displacement in the X direction is 0.53 cm compared to the base isolation system with 7.96 cm and in the Y direction is 0.29 cm compared to 8 cm. The stiffness of shape memory alloys has an insignificant effect on dissipating energy and the relative displacement is slightly different from base isolation systems. According to Figures 14 and 19, the relative displacement difference is negligible in comparison with the base isolation system with the maximum relative displacement of 0.79 cm and 0.67 cm in X and Y direction compared to 0.59 cm and 0.83 cm. The period of the structure is almost same for both cases. The results maximum displacement, residual displacement and maximum relative displacement for three cases of fixed base, isolated base and isolated base equipped with shape memory alloys are listed in Table 5.

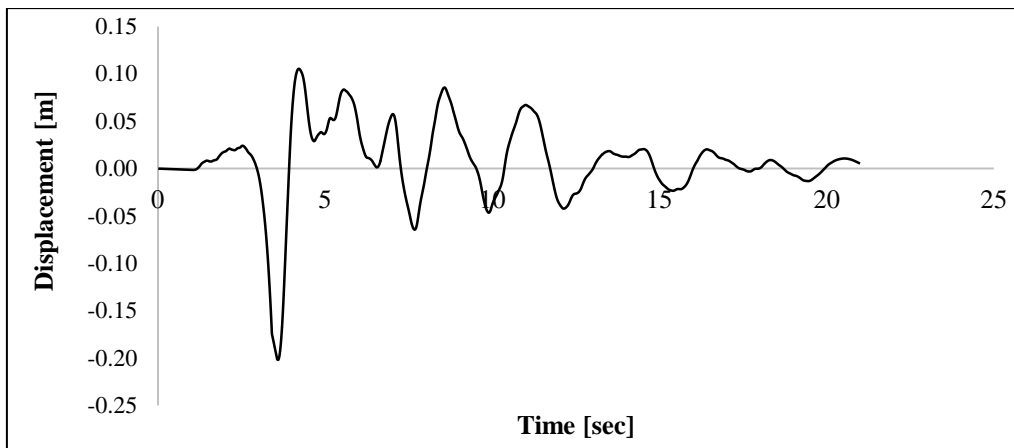


Figure 15. X-Direction displacement response of first floor for Northridge record

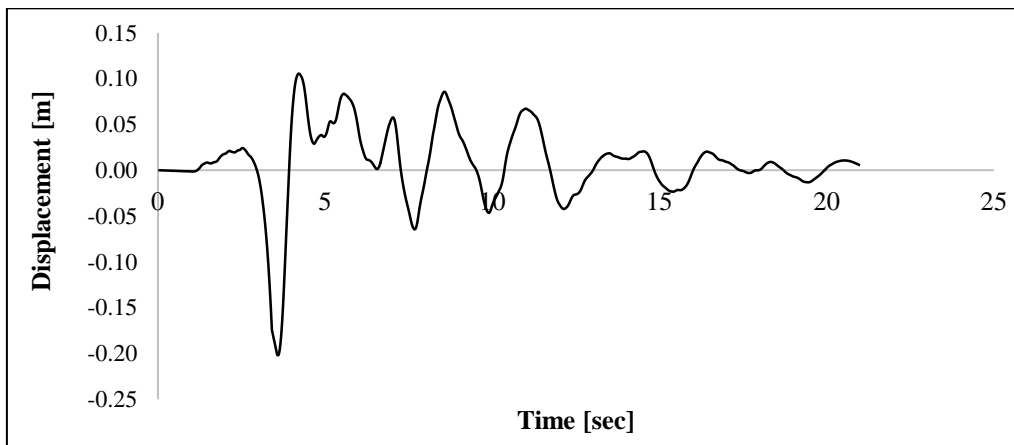


Figure 16. X-Direction displacement response of sixth floor for Northridge record

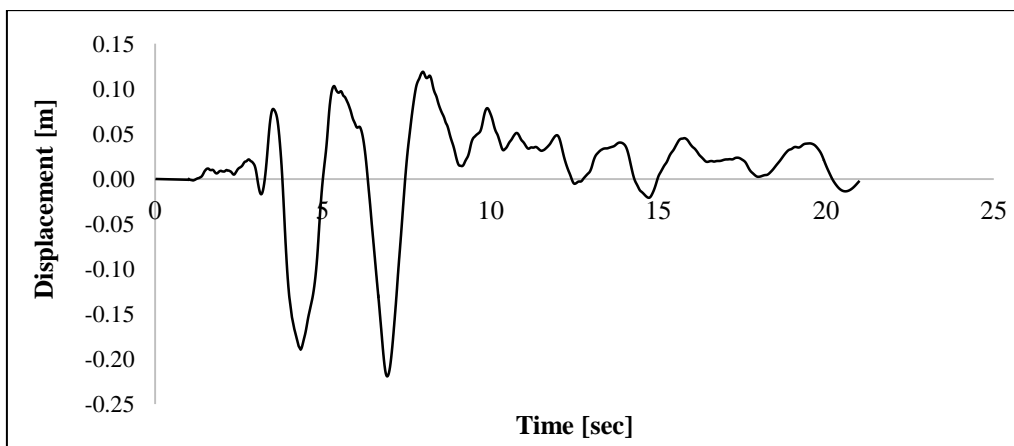


Figure 17. Y-Direction displacement response of first floor for Northridge record

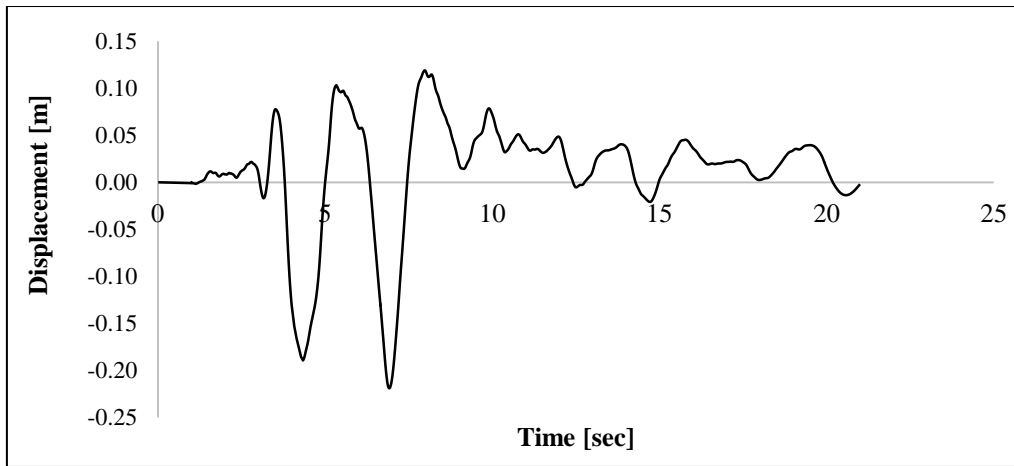


Figure 18. Y-Direction displacement response of sixth floor for Northridge record

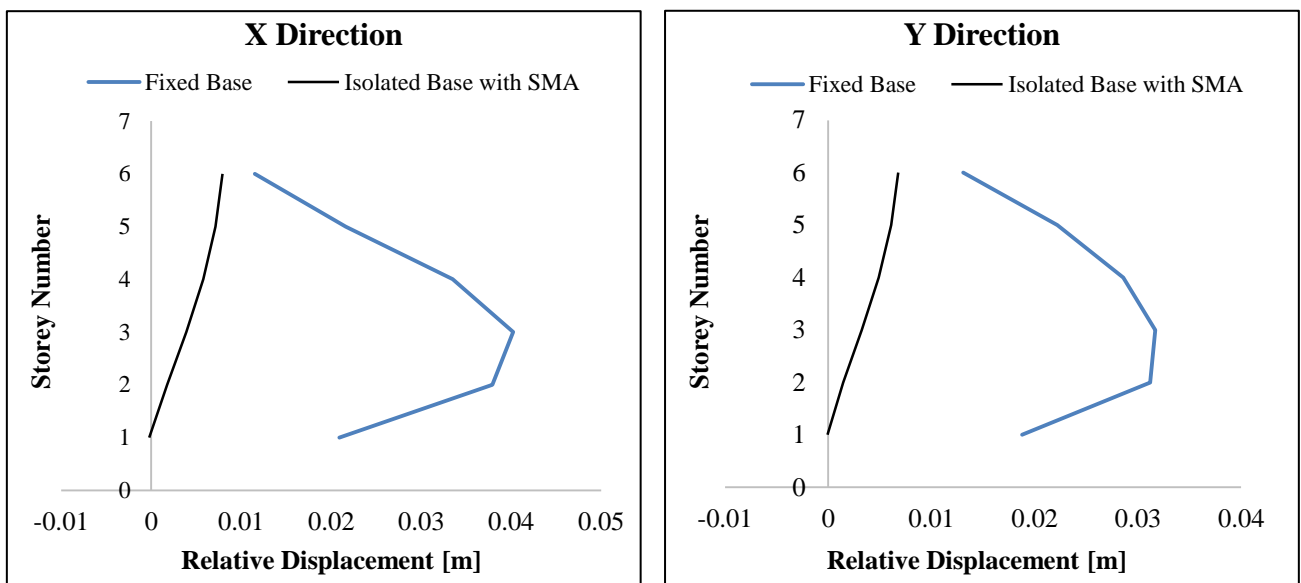


Figure 19. X and Y Direction relative displacement of each floor for Northridge record

Table 5. Results of displacement

	Direction	Storey	Maximum displacement (cm)	Residual displacement (cm)	Decreasing percent	Maximum relative displacement (cm)
Fixed Base	X	Storey 1	2.09	0.11	-	4.02
		Storey 6	17.6	0.12	-	
	Y	Storey 1	1.88	0.18	-	3.17
		Storey 6	19.3	0.14	-	
Isolated Base	X	Storey 1	26.9	7.69	-	0.59
		Storey 6	27.5	7.8	-	
	Y	Storey 1	27.6	8	-	0.83
		Storey 6	28.8	7.6	-	
Isolated Base Equipped with SMA	X	Storey 1	20.1	0.53	93.1%	0.79
		Storey 6	21.5	0.63	91.9%	
	Y	Storey 1	23.5	0.29	96.4%	0.67
		Storey 6	25.6	0.32	95.8%	

5. Conclusion

In this study, a three dimensional six-storey steel structural building was modelled in OpenSees program by locating the isolators under the columns in order to investigate the feasibility of smart isolation systems. Initially, fixed-based results are observed which shows that their responses are same as conventional buildings; with significant storey drifts and vulnerable in near-field earthquake excitations with noticeable acceleration at first story and shear force consequently. Base isolation system results are compared to fixed-based results. Maximum relative displacement of base isolation system has been reduced to 85 percent compared to fixed-based where the period of the structure became 3 times greater than fixed-based structure. Considering the results, in the base-isolated system equipped with shape memory alloys, the residual displacement decreased up to 94 percent in the X direction and up to 97 percent in the Y direction. It can be concluded that the efficient function of a base isolation can be reserved for the future and the maintenance costs of the structure. The importance of the structure and considering the high price of shape memory alloys, the economic values of these types of structures should be considered. The indicated system significantly elevates the durability of base isolation during service level of earthquakes over the time which may reduce base isolation maintenance and replacement expenditures.

6. Conflicts of Interest

The authors declare no conflict of interest.

7. References

- [1] Çerçevik, Ali Erdem, Özgür Avşar, and Oğuzhan Hasançebi. "Optimum Design of Seismic Isolation Systems Using Metaheuristic Search Methods." *Soil Dynamics and Earthquake Engineering* 131 (April 2020): 106012. doi:10.1016/j.soildyn.2019.106012.
- [2] De Luca, Antonello, and Laura Giovanna Guidi. "State of Art in the Worldwide Evolution of Base Isolation Design." *Soil Dynamics and Earthquake Engineering* 125 (October 2019): 105722. doi:10.1016/j.soildyn.2019.105722.
- [3] Markris, Nicos and Mehrdad Aghagholizadeh, "Effect of Supplemental Hysteretic and Viscous Damping on Rocking Response of Free-Standing Columns", *Journal of Engineering Mechanics, ASCE* 145(5), (February 2019). doi:10.1061/(ASCE)EM.1943-7889.0001596.
- [4] Tolani, Sunita, and Ajay Sharma, "Effectiveness of Base-Isolation Technique and Influence of Isolator Characteristics on Response of a Base-Isolated Building", *American Journal of Engineering Research* 5(5), (2016): 198-209.
- [5] Etedali, Sadegh, and Mohammad Reza Sohrabi. "A Proposed Approach to Mitigate the Torsional Amplifications of Asymmetric Base-Isolated Buildings During Earthquakes." *KSCE Journal of Civil Engineering* 20, no. 2 (May 7, 2015): 768–776. doi:10.1007/s12205-015-0325-0.
- [6] Luo, Jie, Larry A. Fahnestock, and James M. LaFave. "Seismic Performance Assessment of Quasi-Isolated Highway Bridges with Seat-Type Abutments." *Journal of Earthquake Engineering* (July 3, 2019): 1–40. doi:10.1080/13632469.2019.1628125.
- [7] Xiang, Nailiang, M. Shahría Alam, and Jianzhong Li. "Yielding Steel Dampers as Restraining Devices to Control Seismic Sliding of Laminated Rubber Bearings for Highway Bridges: Analytical and Experimental Study." *Journal of Bridge Engineering* 24, no. 11 (November 2019): 04019103. doi:10.1061/(asce)be.1943-5592.0001487.
- [8] Hurlbaas, S., and L. Gaul. "Smart Structure Dynamics." *Mechanical Systems and Signal Processing* 20, no. 2 (February 2006): 255–281. doi:10.1016/j.ymsp.2005.08.025.
- [9] Wesolowsky, Michael J. and John C. Wilson, "Controlling Seismic Response with Shape Memory Alloy Devices" 13th World Conference on Earthquake Engineering, Vancouver, Canada, (August 2004), Paper No. 949.
- [10] Asgharian, Behrouz, Neda Salari, and Behnam Saadati, "Application of Intelligent Passive Devices based on Shape Memory Alloys in Seismic Control Structures", *Structures* 5, (February 2016): 161-169. doi:10.1016/j.istruc.2015.10.013.
- [11] Tian, Li, Guodong Gao, Canxing Qiu, and Kunjie Rong. "Effect of Hysteresis Properties of Shape Memory Alloy-Tuned Mass Damper on Seismic Control of Power Transmission Tower." *Advances in Structural Engineering* 22, no. 4 (August 9, 2018): 1007–1017. doi:10.1177/1369433218791606.
- [12] Ghasemi, Mohammad Reza, Naser Shabakhty, and Mohammad Hadi Enferadi. "Vibration Control of Offshore Jacket Platforms through Shape Memory Alloy Pounding Tuned Mass Damper (SMA-PTMD)." *Ocean Engineering* 191 (November 2019): 106348. doi:10.1016/j.oceaneng.2019.106348.
- [13] Rahgozar, Peyman, "Free Vibration of Tall Buildings using Energy Method and Hamilton's Principle" *Civil Engineering Journal* 6.5 (April 2020): 945-953. doi:10.28991/cej-2020-03091519.

- [14] Kamgar, Reza, and Peyman Rahgozar, "Reducing Static Roof Displacement and Axial Forces of Columns in Tall Buildings Based on Obtaining the Best Locations for Multi-Rigid Belt Truss Outrigger Systems." *Asian Journal of Civil Engineering* 20.6 (April 2019): 759–768. doi:10.1007/s42107-019-00142-0.
- [15] Nakashima, Masayoshi, Peng Pan, Dan Zamfirescu, and Ruediger Weitzmann, "Post-Kobe Approach for Design and Construction of Base-Isolated Buildings." *Journal of Japan Association for Earthquake Engineering* 4.3 (January 2004): 259-264. doi:10.5610/jaee.4.3_259.
- [16] Maldonado-Mercado, Julio Cesar, "Passive and Active Control of Structures." Thesis for Master of Science, Massachusetts Institute of Technology, (May 1995).
- [17] Naeim, Farzad, and James M. Kelly, "Design of Seismic Isolated Structures: From Theory to Practice." John Wiley & Sons (5 March 1999): doi:10.1002/9780470172742.
- [18] Chan Win, Aung, "Analysis and Design of Base Isolation for Multi-Storied Building." *International Conference on Sustainable Development*, (November 2008): 18-19. doi:10.1155/2014/585429.
- [19] Tafheem, Zasiyah, Tanvir Ahmed Arafat, Amlan Chowdhury, and Ashique Iqbal. "Seismic Isolation Systems in Structures-the State of Art Review." In *Proceedings of 11th Global Engineering, Science and Technology Conference*, (December 2015):18-19.
- [20] Islam, Saiful, Raja Rizwan Hussain, Mohd Zamin Jumaat, and Muhammad Ashique Rahman, "Nonlinear Dynamically Automated Excursions for Rubber-Steel Bearing Isolation in Multi-Storey Construction." *Automation in Construction* 30 (March 2013): 265-275. doi:10.1016/j.autcon.2012.11.010.
- [21] ASCE/SEI 7-16. "Minimum Design Loads and Associated Criteria for Buildings and other Structures." Reston, VA: American Society of Civil Engineers (2017).